High-Capacity, Protein-Binding Membranes Based on Polymer Brushes Grown in Porous Substrates

Lei Sun, Jinhua Dai, Gregory L. Baker,* and Merlin L. Bruening*

Department of Chemistry, Michigan State University, East Lansing, Michigan 48824

Received March 7, 2006. Revised Manuscript Received May 22, 2006

The use of atom transfer radical polymerization to grow poly(2-hydroxyethyl methacrylate) (PHEMA) brushes in porous alumina followed by functionalization of the PHEMA with nitrilotriacetate−Cu^{2+} complexes yields membranes that adsorb proteins via coordination of Cu^{2+} to histidine residues. Adsorption isotherms show that these membranes have binding capacities as high as 0.9 mg of bovine serum albumin (BSA)/cm^2 of external membrane surface area (150 mg/cm^3 of membrane), and breakthrough curves indicate that saturation of the membranes with BSA or myoglobin occurs in less than 15 min. The efficiency of protein elution with ethylenediaminetetraacetic acid (EDTA) solutions is essentially 100%, and the membranes show no detectable decrease in capacity over nine cycles of binding, elution, and regeneration with Cu^{2+}. The unusually high capacity of these membranes for rapid protein binding makes them attractive for applications such as purification of His-tag proteins.

Introduction

Potential therapeutic applications of proteins along with rapid developments in biotechnology and genetic engineering have greatly increased the rate of production of various proteins and enzymes.[1,2] Accompanying this increase in the scale of protein production is a need for fast and convenient purification techniques. Affinity chromatography is probably the most convenient way to purify proteins due to its ability to separate biomolecules on the basis of their biological interactions,[2,3] but the rate of separations with packed-bead affinity columns is limited by slow diffusion of biomacromolecules within bead pores.[3−5]

Affinity membrane chromatography, which was initially introduced by Henis et al. in 1987,[6] has the potential to overcome this disadvantage of packed-bead columns because the protein solutions being treated must flow through the membrane pores.[7−9] Additionally, membrane chromatography avoids challenges in packing of columns, which makes it an attractive technique for large-scale separation processes. A number of adsorptive membranes are now available commercially,[10] and a wide range of porous materials such as cellulose,[11] chitin,[12,13] chitosan,[14] and nylon[15] have been used as substrates that can be modified for protein immobilization.

Despite their potential, the major disadvantage of membrane absorbers is their low binding capacity relative to beads. The specific surface area of membranes is simply not as great as that of beads. This can be overcome to some extent through the use of polymer chains grafted in membrane pores and binding of multilayers of proteins to these polymers. For example, Ulbricht and Yang[16] achieved a lysozyme-binding capacity of 20 mg/cm^3 by grafting poly(acrylic acid) to polypropylene membranes modified with adsorbed photoinitiators.

This research aims at utilizing the controlled growth of polymer brushes in porous supports to develop affinity membranes with remarkably high protein-binding capacities. The use of atom transfer radical polymerization (ATRP) to grow poly(2-hydroxyethyl methacrylate) (PHEMA) from initiators bound to a porous alumina surface affords relatively fine control over polymer molecular weight, which allows large increases in capacity without clogging of membrane pores. PHEMA brushes are particularly attractive because they can be functionalized to exploit a number of affinity interactions.[17−19] Specifically, functionalization of PHEMA with nitrilotriacetate−Cu^{2+} complexes results in protein binding via metal-ion affinity interactions, and a microporous

* To whom correspondence should be addressed: phone (517) 355-9715, ext 237; fax (517) 353-1793; e-mail bruening@cem.msu.edu.

(1) Arica, M. Y.; Testereci, H. N.; Denizli, A. *J. Chromatogr. A* **1998**, *799*, 83.
(2) Kawai, T.; Saito, K.; Lee, W. *J. Chromatogr. B* **2003**, *790*, 131.
(3) Zou, H.; Luo, Q.; Zhou, D. *J. Biochem. Biophys. Methods* **2001**, *49*, 199.
(4) Clairbois, A. S.; Letourneur, D.; Muller, D.; Jozefonvicz, J. *J. Chromatogr. B* **1998**, *706*, 55.
(5) Sun, G.-Y.; Shi, Q.-H.; Sun, Y. *J. Chromatogr. A* **2004**, *1061*, 159.
(6) Henis, J. M. S.; Tripodi, M. K.; Stimpson, D. I. European Patent 0,-221,046B1, October 30, 1987.
(7) Charcosset, C. *J. Chem. Technol. Biotechnol.* **1998**, *71*, 95.
(8) Urmenyi, A. M.; Poot, A. A.; Wessling, M.; Mulder, M. H. V. *J. Membr. Sci.* **2005**, *259*, 91.
(9) Wu, C.-Y.; Suen, S.-Y.; Chen, S.-C.; Tzeng, J.-H. *J. Chromatogr. A* **2003**, *996*, 53.
(10) Roper, D. K.; Lightfoot, E. N. *J. Chromatogr. A* **1995**, *702*, 3.
(11) Sarfert, F. T.; Etzel, M. R. *J. Chromatogr. A* **1997**, *764*, 3.
(12) Ruckenstein, E.; Zeng, X. *Biotechnol. Bioeng.* **1997**, *56*, 610.
(13) Zeng, X.; Ruckenstein, E. *J. Membr. Sci.* **1999**, *156*, 97.
(14) Zeng, X.; Ruckenstein, E. *J. Membr. Sci.* **1996**, *117*, 271.
(15) Castilho, L. R.; Deckwer, W. D.; Anspach, F. B. *J. Membr. Sci.* **2000**, *172*, 269.
(16) Ulbricht, M.; Yang, H. *Chem. Mater.* **2005**, *17*, 2622.
(17) Sun, L.; Baker, G. L.; Bruening, M. L. *Macromolecules* **2005**, *38*, 2307.
(18) Miller, M. D.; Baker, G. L.; Bruening, M. L. *J. Chromatogr. A* **2004**, *1044*, 323.
(19) Bayramoglu, G.; Yilmaz, M.; Arica, M. Y. *Colloids Surf., A* **2004**, *243*, 11.

10.1021/cm060554m CCC: $33.50
Published on Web 07/19/2006

alumina support provides a ~500-fold increase in surface area relative to two-dimensional supports. Overall, the combination of the alumina supports and functionalized polymer brushes yields a remarkable binding capacity of 0.9 mg of bovine serum albumin (BSA)/cm^2 of external membrane surface (150 mg/cm^3 of membrane). Previously reported membrane absorbers have protein capacities of 4−20 mg/cm^3.[16,20,21]

A few recent studies demonstrated the possibility of using ATRP and other polymerization techniques to prepare protein-adsorbing polymer brushes.[2,16,22−24] Matyjaszewski and co-workers[22] reported electrostatic adsorption of 10 to 15 monolayers of BSA to poly(dimethylamino ethyl methacrylate) brushes grown on flat surfaces. Husson and co-workers[25] used ATRP to prepare poly(2-vinylpyridine) brushes in porous poly(vinylidene difluoride). Although these brushes were reported to enhance lysozyme adsorption, no capacity was provided. The PHEMA-modified membranes described here clearly demonstrate the advantages of polymer brushes for membrane-based affinity separations.

Experimental Section

Materials. Anodisc porous alumina membranes with 0.2 μm diameter surface pores were obtained from Fisher Scientific. Scanning electron microscopy (SEM) images suggest that pore diameters in the bulk of these membranes are about 0.25 μm. Dimethylformamide (DMF, anhydrous, 99.8%), 11-mercaptoundecanol (97%), 2-bromoisobutyryl bromide (98%), CuCl (99.999%), $CuBr_2$ (99%), 2,2′-bipyridyl (bpy, 99%), 1-[3-(dimethylamino)-propyl]-3-ethylcarbodiimide hydrochloride (EDC), *N*-hydroxysuccinimide (NHS), 4-(dimethylamino)pyridine (DMAP), ethylenediaminetetraacetic acid (EDTA), bovine serum albumin (BSA), and myoglobin were used as received from Sigma−Aldrich. $CuSO_4 \cdot 5H_2O$ (Columbus Chemical), N_α,N_α-bis(carboxymethyl)-L-lysine hydrate (Fluka, aminobutyl-NTA), succinic anhydride (SA, Matheson Coleman & Bell), and Coomassie protein assay reagent (Pierce) were also used as received. 2-Hydroxyethyl methacrylate (HEMA, Aldrich, 97%, inhibited with 300 ppm hydroquinone monomethyl ether) was purified by passing it through a column of activated basic alumina (Spectrum), and the trichlorosilane initiator (11-[(2-bromo-2-methyl)propionyloxy]undecyltrichlorosilane) was synthesized according to a literature procedure.[26] Buffers were prepared from analytical-grade chemicals and deionized (Milli-Q, 18.2 MΩ·cm) water.

Polymerization of HEMA in Porous Alumina Membranes and on Au Substrates. The alumina membrane was first cleaned in a UV/ozone cleaner (Boekel model 135500) for 12 min and sandwiched inside a membrane cell (Millipore, Swinnex 25). A Masterflex 7518-60 peristaltic pump was used to circulate 1 mM trichlorosilane initiator in DMF through the membrane for 3 h at a rate of 10 mL/min, and subsequent rinsing with ethanol (20 mL), water (20 mL), and acetone (20 mL) at a flow rate of 10 mL/min yielded an initiator-modified membrane. Polymerization of HEMA occurred by circulating a solution containing 15 mL of purified HEMA, 15 mL of methanol, 82.5 mg (0.825 mmol) of CuCl, 54 mg (0.24 mmol) of $CuBr_2$, and 320 mg (2.04 mmol) of bpy through the initiator-modified membrane by use of a peristaltic pump (7 mL/min) for 1 h. This HEMA solution was initially degassed via three freeze−pump−thaw cycles and prepared as described previously.[17] After polymerization, the membrane was cleaned by flowing ethanol (20 mL), water (20 mL), and acetone (20 mL) through the membrane at 7 mL/min.

To prepare films for reflectance FTIR characterization, Au-coated silicon wafers were coated with a mercaptoundecanol monolayer that was subsequently derivatized with 2-bromoisobutyryl bromide as described previously.[27,28] Polymerization of HEMA from these substrates occurred as described above, except the substrate was simply immersed in a polymerization solution that was kept in a glovebag.

PHEMA Derivatization and Protein Immobilization. To derivatize PHEMA-coated alumina membranes, a 55 °C DMF solution containing SA (10 mg/mL) and DMAP (15 mg/mL) was first passed through the membrane for 3 h at 7 mL/min, followed by rinsing with DMF (20 mL), water (20 mL), and ethanol (20 mL) at 7 mL/min (Scheme 1). Next, a room-temperature solution containing EDC/NHS (0.1 M each in pure water) was circulated for 30 min (6.8 mL/min) through the membrane, which was then briefly washed with water and ethanol (20 mL each). The EDC/NHS-activated membrane was then reacted with a 0.1 M aminobutyl-NTA solution (adjusted to pH 10.2) for 1 h at 6.5 mL/min, rinsed with 20 mL of water, and finally exposed to a 0.1 M $CuSO_4$ solution (6.5 mL/min) for 30 min and rinsed with 20 mL of water. The membrane was then taken out of the Swinnex 25 cell, rinsed sequentially with 5 mL of water, ethanol, and acetone by use of a pipet, and dried with a flow of nitrogen. The water remaining in the pump tubing was then pumped out, and the membrane was put back into the cell. A solution containing BSA or myoglobin (in 20 mM pH 7.2 phosphate buffer) was next forced through the membrane, and the permeate was collected for analysis at specific time intervals. Permeate volume was estimated by use of a graduated cylinder. Subsequently, the membrane was rinsed with pH 7.2 phosphate buffer, and protein was eluted with a 50 mM EDTA solution (pH adjusted to 7.2). To prepare films for reflectance FTIR characterization, a PHEMA film on a gold substrate was treated in a similar procedure by immersing the substrate in appropriate solutions and rinsing with solutions from a pipet.

Determination of Protein Concentrations. To determine the concentration of protein in permeate and eluent solutions, 50 μL of the sample was added to 2.95 mL of a solution of Coomassie reagent, and the mixture was shaken a few times and allowed to react for 5 min at room temperature. The UV/vis absorbance spectra of these solutions were then obtained with a Perkin-Elmer UV/vis (model Lambda 40) spectrophotometer. Calibration curves for the absorbance of BSA and myoglobin/Coomassie solutions at 595 nm were obtained for a series of protein solutions (concentration range of 100 μg−2 mg of protein/mL) that were mixed with Coomassie reagent. All spectra were measured against a Coomassie reagent background.

(20) Guo, W.; Ruckenstein, E. *J. Membr. Sci.* **2003**, *215*, 141.
(21) Kubota, N.; Nakagawa, Y.; Eguchi, Y. *J. Appl. Polym. Sci.* **1996**, *62*, 1153.
(22) Kusumo, A.; Bombalski, L.; Qiao, L.; Kowalewski, T.; Matyjaszewski, K.; Schneider, J. W.; Tilton, R. D. AIChe Annual Meeting, Cincinnati, OH, 2005, *01C14*, 123d.
(23) Ito, H.; Nakamura, M.; Saito, K.; Sugita, K.; Sugo, T. *J. Chromatogr. A* **2001**, *925*, 41.
(24) Okamura, D.; Sait, K.; Sugita, K.; Tamada, M.; Sugo, T. *J. Chromatogr. A* **2002**, *953*, 101.
(25) Singh, N.; Husson, S. M.; Zdyrko, B.; Luzinov, I. *J. Membr. Sci.* **2005**, *262*, 81.
(26) Matyjaszewski, K.; Miller, P. J.; Shukla, N.; Immaraporn, B.; Gelman, A.; Luokala, B. B.; Siclovan, T. M.; Kickelbick, G.; Vallant, T.; Hoffmann, H.; Pakula, T. *Macromolecules* **1999**, *32*, 8716.
(27) Kim, J.-B.; Bruening, M. L.; Baker, G. L. *J. Am. Chem. Soc.* **2000**, *122*, 7616.
(28) Kim, J.-B.; Huang, W.; Bruening, M. L.; Baker, G. L. *Macromolecules* **2002**, *35*, 5410.

Scheme 1. Derivatization of PHEMA for Protein Immobilization

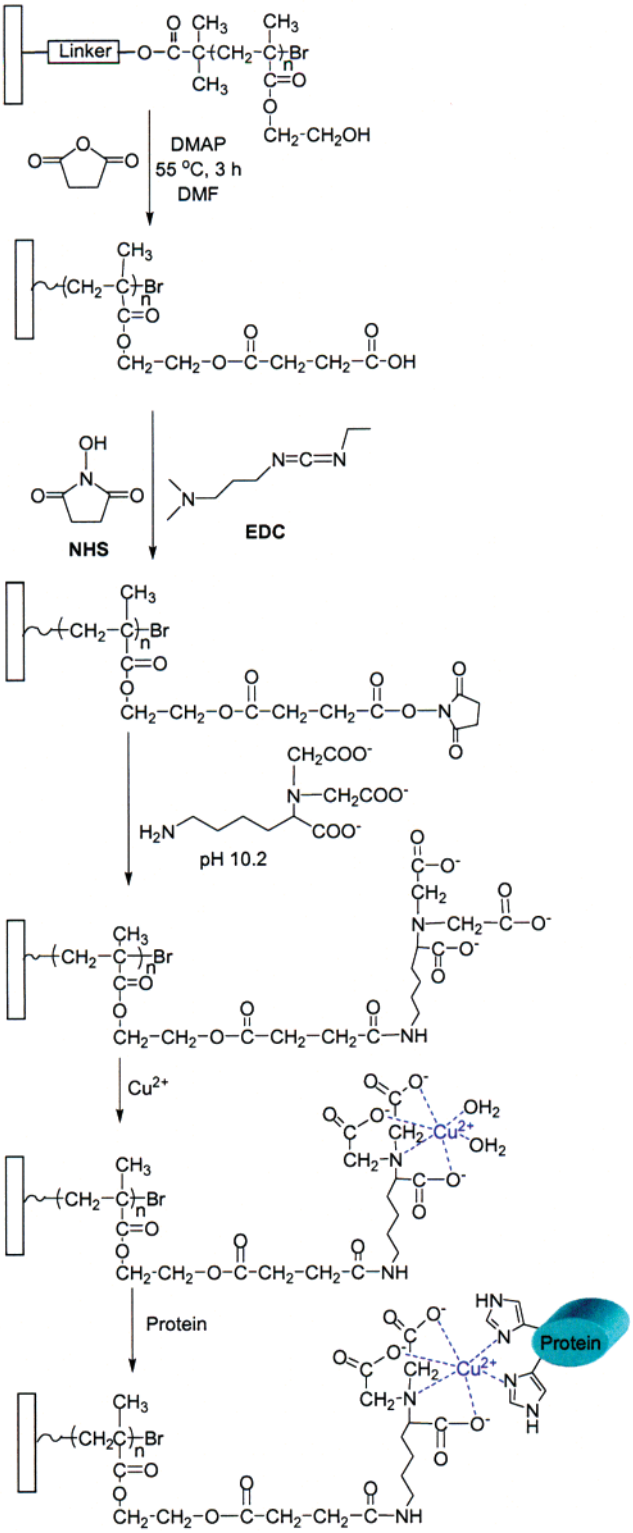

Film Characterization Methods. Film growth inside alumina membranes was verified by field-emission scanning electron microscopy (FESEM, Hitachi S-4700II, acceleration voltage of 15 kV) and energy-dispersive X-ray spectroscopy (EDS, Phoenix EDAX instrument). For SEM and EDS observations, the alumina membrane was attached to a Si wafer by double-sided tape, and the alumina was dissolved by immersing it into 1 M NaOH at 25 °C for 2 h, followed by careful washing several times with distilled water and ethanol. Subsequently, 7 nm of gold was sputtered onto the remaining polymer prior to FESEM and EDS examination. Reflectance FTIR spectra of films on gold-coated wafers were obtained on a Nicolet Magna-IR 560 instrument with a Pike grazing angle (80°) accessory. The spectrum of reflection from a UV/ozone-cleaned, gold-coated wafer was used as a background.

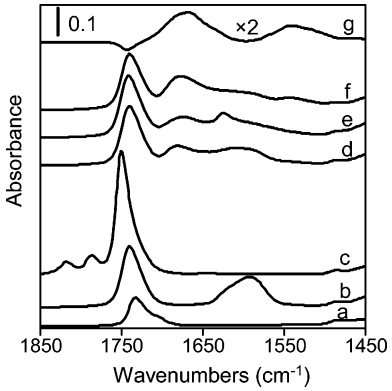

Figure 1. Reflectance FTIR spectra of a PHEMA film before (a) and after the following sequential steps: (b) reaction with SA, immersion in a pH 9.9 buffer, and rinsing with ethanol; (c) activation with EDC/NHS; (d) reaction with aminobutyl NTA followed by immersion in pH 9.9 buffer; (e) exposure to 0.1 M Cu^{2+} to form NTA−Cu^{2+} complexes; (f) exposure to 1 mg/mL BSA followed by immersion in pH 9.9 buffer. Spectrum g is the difference spectrum resulting from subtraction of d from f and multiplication by a factor of 2.

Results and Discussion

FTIR Characterization of PHEMA Derivatization and Protein Binding. Reflectance FTIR spectra of PHEMA films and their derivatives on Au-coated Si confirm the steps of the derivatization and protein-adsorption procedure shown in Scheme 1. To prepare brushes capable of protein binding, we first reacted PHEMA with SA to create free -COOH groups in the film. Prior to obtaining the reflectance IR spectrum of SA-derivatized films, we immersed the film-coated gold slide in pH 9.9 buffer for 15 min and rinsed with ethanol. At pH 9.9, the newly introduced carboxylic acid groups should be deprotonated,[29] and consistent with derivatization and deprotonation, the FTIR spectrum of these films contains a new peak around 1594 cm^{-1} (Figure 1b), which is likely due to the -COO^- symmetric stretch. The absorbance at ∼1740 cm^{-1}, which is assigned to ester carbonyl groups, approximately doubled after SA derivatization, suggesting a high degree of conversion of the -OH groups of PHEMA to ester groups. The disappearance of the -OH stretch of PHEMA (3650−3100 cm^{-1}; Figure 1, Supporting Information) also indicates nearly 100% derivatization.

After activation of the -COOH groups of modified PHEMA with EDC/NHS, peaks due to the succinimide ester appeared at 1817 and 1786 cm^{-1} (Figure 1c).[30−32] The asymmetric stretch of succinimide (∼1753 cm^{-1}) overlaps with the C═O stretch (1740 cm^{-1}) of the previously formed esters to yield a broad peak with an absorbance that is about

(29) Hong, Y. K.; Hong, W. H. *Sep. Purif. Technol.* **2005**, *42*, 151.
(30) Dordi, B.; Schoenherr, H.; Vancso, G. J. *Langmuir* **2003**, *19*, 5780.
(31) Lahiri, J.; Isaacs, L.; Tien, J.; Whitesides, G. M. *Anal. Chem.* **1999**, *71*, 777.
(32) Xiao, S.-J.; Brunner, S.; Wieland, M. *J. Phys. Chem. B* **2004**, *108*, 16508.

double that for the ester carbonyl after SA derivatization. The new peak at 1817 cm^{-1} is due to the carbonyl stretch of the active ester formed by reaction with NHS, while the absorbance at 1786 cm^{-1} results from the symmetric succinimide stretch.[30−32]

The EDC/NHS-activated PHEMA was then reacted with aminobutyl-NTA [N_α,N_α-bis(carboxymethyl)-L-lysine hydrate], immersed in pH 9.9 buffer for 15 min, and rinsed with ethanol. Reaction of the activated ester with both aminobutyl-NTA and water resulted in the loss of the active ester absorbances and the shift of the 1753 cm^{-1} peak back to 1740 cm^{-1} (Figure 1d). The new peak at 1680 cm^{-1} provides evidence for NTA immobilization and is probably due to the COO^- groups from NTA as well as the amide bond formed during aminobutyl-NTA attachment. The broad absorbance centered at 1600 cm^{-1} could result from carboxylate groups in either NTA or the hydrolyzed active esters. Exposure of NTA-derivatized PHEMA to 0.1 M $CuSO_4$ followed by rinsing with water yielded immobilized NTA−Cu^{2+} that is capable of binding proteins through their histidine groups. Unfortunately, there was no significant change in the IR spectrum (Figure 1e) of the film after Cu^{2+} coordination except that the peak at 1600 cm^{-1} appeared to shift to 1630 cm^{-1} and become sharper. However, this shift could be due to the fact that spectrum d was measured after treatment with pH 9.9 buffer, while the sample for spectrum e was not treated with this buffer because $Cu(OH)_2$ might precipitate in the film at high pH. XPS data confirmed the presence of Cu^{2+} in the film and showed a Cu:N ratio of 0.4:1, which is consistent with our previous results and indicative of nearly one Cu^{2+} per NTA moiety.[33]

After an overnight exposure of the PHEMA−NTA−Cu^{2+} film to a 1 mg/mL BSA solution in pH 7.2 buffer followed by immersion in pH 9.9 buffer for 15 min and rinsing in EtOH, we saw growth in the absorbance at 1680 cm^{-1} (amide I band) and the appearance of a small peak at 1545 cm^{-1} (amide II band) (Figure 1f). Subtracting the spectrum of PHEMA−NTA (Figure 1d) from that of PHEMA−NTA−Cu^{2+}−BSA (Figure 1f) yielded a bound-BSA spectrum, which is dominated by amide absorbances (Figure 1g). We chose to subtract the PHEMA−NTA rather than the PHEMA−NTA−Cu^{2+} spectrum because the former was taken after immersion in a pH 9.9 buffer, as was the spectrum of PHEMA−NTA−Cu^{2+}−BSA. Comparison of the amide intensities in Figure 1g with those of spin-coated films of pure BSA suggests that about 40 nm of BSA adsorbed to this film.[33] Assuming a monolayer height of 4.0 nm,[34] this thickness corresponds to 10 monolayers of bound BSA. The PHEMA film was initially 50 nm thick.

SEM and EDS Characterization of PHEMA inside Alumina Membranes. In our previous research, we used ATRP to graft PHEMA from the surface of porous alumina substrates and form composite membranes with ultrathin PHEMA skins.[17] In contrast, this work aimed at grafting PHEMA within the pores of the membrane to achieve a high surface area for protein capture. By pumping the initiator and monomer solutions through the membrane, we were able to achieve polymerization throughout the support and increase the surface area from which polymerization occurred by 500-fold. One challenge in such polymerizations is to grow polymer brushes without clogging the membrane. To overcome this difficulty, we used methanol instead of water as the solvent for brush growth to decrease the rate of polymerization.

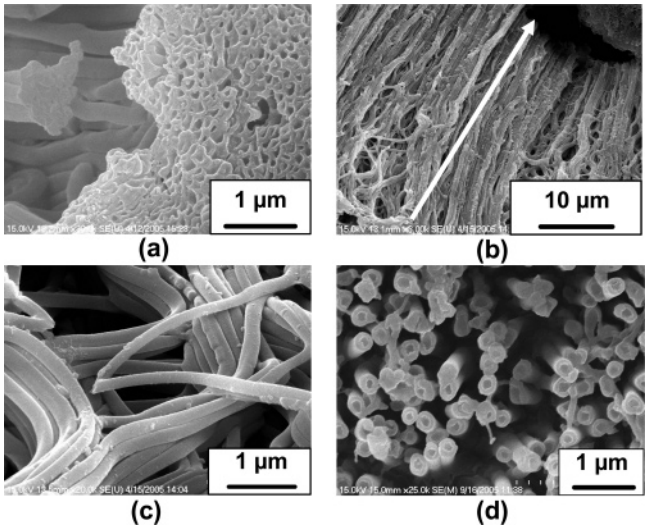

Figure 2. FESEM images of PHEMA nanotubes synthesized by ATRP in porous alumina substrates. (a) Top view of the nanotubes. (b) Cross-sectional image showing the length of the nanotubes. (c) Highly flexible PHEMA nanotubes. (d) Top view of the nanotubes obtained by removing the surface layer by polishing with sand paper. The arrow in panel b shows the approximate length of the tubes.

The SEM images in Figure 2 clearly demonstrate the formation of hollow PHEMA tubes in the membrane pores.[35,36] To obtain these images, we dissolved the alumina template in 1 M NaOH and collected the polymer tubes before the SEM images were taken. (PHEMA likely does not dissolve in 1 M NaOH because it is lightly cross-linked.[37]) The right side of Figure 2a shows an image of the top of the brushes, which is similar to images of bare porous alumina. Figure 2b indicates that the length of the resulting nanotubes is about 45 μm, which is slightly less than the thickness of the alumina support (60 μm), perhaps because the tubes curled up. Figure 2c shows the flexibility of the tubes. The image in Figure 2d was obtained after removal of the skin layer of the membrane by polishing with sandpaper to expose the interior of the pores. (Although Figure 2a shows that the pores are open at the surface of the membrane, it does not necessarily imply that the interior of the pores is open.) Figure 2d shows open, interior pores, but the thickness of the polymers is much higher than what we calculated from flow experiments (see below). Because the sanding process may cause the pores to appear thicker than they are, we do not think that Figure 2d can be employed to determine the inner diameter of the tubes. The energy-dispersive X-ray spectrum of the nanotubes (Figure 2,

(33) Dai, J.; Bao, Z.; Sun, L.; Hong, S. U.; Baker, G. L.; Bruening, M. L. *Langmuir* **2006**, *22*, 4274.
(34) Tsuneda, S.; Saito, K.; Furusaki, S.; Sugo, T. *J. Chromatogr. A* **1995**, *689*, 211.
(35) Hou, S.; Wang, J.; Martin, C. R. *J. Am. Chem. Soc.* **2005**, *127*, 8586.
(36) Martin, C. R. *Science* **1994**, *266*, 1961.
(37) Huang, W.; Kim, J.-B.; Bruening, M. L.; Baker, G. L. *Macromolecules* **2002**, *35*, 1175.

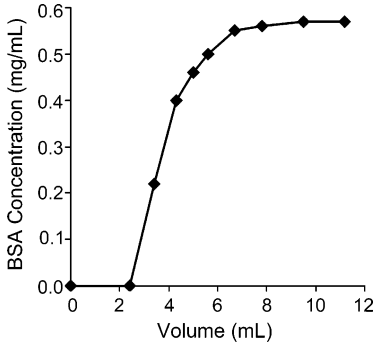

Figure 3. Breakthrough curve for BSA adsorption in porous alumina membranes coated with PHEMA−NTA−Cu^{2+}. The BSA concentration in the feed solution was 0.56 mg/mL and the initial flow rate was 2.4 mL/min, decreasing to 0.9 mL/min at the end of the experiment.

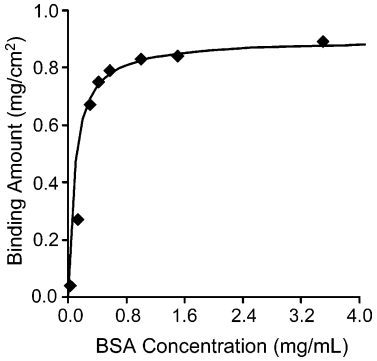

Figure 4. Equilibrium binding capacity of PAA−NTA−Cu^{2+}-coated alumina membranes as a function of BSA concentration. The solid line represents the fit of the data to the Langmuir isotherm.

Supporting Information) reveals C and O and not Al, demonstrating that these images are indeed those of PHEMA.

BSA Binding to PHEMA−NTA−Cu^{2+} Brushes. To test the binding capacity of PHEMA−NTA−Cu^{2+} films, we initially pumped a 0.56 mg/mL BSA solution through the membrane, collected the permeate over specific time intervals, and analyzed these solutions by their absorbance at 595 nm in a Bradford assay. Figure 3 of the Supporting Information presents typical UV−vis spectra from the Bradford assays. The breakthrough curve (Figure 3) obtained from these measurements shows that essentially all of the BSA was adsorbed until breakthrough occurred and that saturation of the membrane took less than 15 min.[34,38,39] Integration of the difference between the feed concentration and the concentrations given in Figure 3 gives a remarkable 0.8 mg of bound BSA/cm^2 of external membrane surface area. Repetition of this experiment on four different membranes yielded an average BSA binding of 0.82 ± 0.07 mg/cm^2. This very high capacity is due in part to the high internal surface area of the alumina, but even when the surface area of the pores is taken into account (assuming 50% porosity, pore diameters of 0.25 μm, and a membrane thickness of 60 μm), the capacity is 1.6 μg of BSA/cm^2 of pore area. This corresponds to ∼4 monolayers of BSA (assuming a BSA density of 1 g/cm^3 and a monolayer thickness of 4.0 nm) adsorbed throughout the pores of these membranes.

Figure 4 shows how the amount of equilibrium binding of BSA to PHEMA−NTA−Cu^{2+} films in alumina membranes varies with the concentration of BSA. In this experiment, binding was performed at a specific BSA concentration, and the membrane was regenerated with 0.05 M EDTA (pH 7.2) followed by 0.1 M Cu^{2+} prior to examination of adsorption at another BSA concentration. As can be seen, BSA binding increases with its concentration in the feed solution until it approaches saturation at concentrations around 1 mg/mL. The data are reasonably described by the Langmuir isotherm,[9,40−42] $q = q_m C/(K_d + C)$, where q is the amount of protein bound, q_m represents the saturation capacity, C is the concentration of protein in solution, and K_d is the dissociation equilibrium constant. The value of q_m determined from the Langmuir plot is 0.9 mg/cm^2 of external membrane surface area, and the dissociation constant is 0.09 mg/mL, which also corresponds to 1.3 μM. This K_d value is reasonably consistent with the previously reported value of 2.3 μM for chitosan−Cu^{2+}−BSA[43] and indicates a strong binding affinity between BSA and immobilized NTA−Cu^{2+} complexes.

The high protein-binding capacity of these membranes is also consistent with decreases in flow rate after protein binding. As noted in Figure 3, flow rate decreased from 2.4 to 0.9 mL/min during binding of 0.8 mg of BSA/cm^2 of external membrane surface area (130 mg/cm^3). We achieved a similar decrease in flow rate when we loaded protein in the membrane using a dead-end filtration cell (Millipore, Model 8010) with a controlled pressure of 6.9×10^4 pascals (10 psig). Assuming Poiseuille flow in the membranes (flow rate is proportional to pore radius raised to the 4th power), the drop in flow rate suggests that the radius of the membrane pores decreased by a factor of 1.28 after protein binding. If an open pore radius of 0.112 μm after PHEMA−NTA−Cu^{2+} deposition is used (see below) and a 50% porosity prior to film deposition is assumed, the decrease in radius by a factor of 1.28 upon protein binding would yield a decrease in pore volume of 0.16 cm^3/cm^3 of total membrane. With a protein density of 1 g/cm^3, this decrease in pore volume agrees well with both the BSA binding capacity of 130 mg/cm^3 for the membrane used to obtain Figure 3 and the saturated binding capacity of 150 mg/cm^3 (Figure 4). Thus, the high protein-binding capacity is consistent with the flow rates through the membrane.

Flow rates before polymerization and after deposition of PHEMA−NTA−Cu^{2+} were 10 and 6.5 mL/min, respectively, suggesting that the pore radius decreased from 0.125 μm before polymerization (radius estimated from FESEM images) to 0.112 μm after deposition of the PHEMA−NTA−Cu^{2+} film. This implies a film thickness of 12 nm, which appears to be less than that in the SEM images of PHEMA tubes in Figure 2, but as mentioned previously, the polymers might be much thicker at their surface than in the bulk of the membrane. We should note that flow rate dropped from 6.5 to 2.5 mL/min almost instantaneously when we began

(38) Shi, W.; Zhang, F.; Zhang, G. *J. Chromatogr. A* **2005**, *1081*, 156.
(39) Hao, W.; Wang, J. *Chromatographia* **2005**, *62*, 55.
(40) Iwats, H.; Saito, K.; Furusaki, S. *Biotechnol. Prog.* **1991**, *7*, 412.
(41) Arica, M. Y.; Denizli, A.; Salih, B.; Piskin, E.; Hasirci, V. *J. Membr. Sci.* **1997**, *129*, 65.
(42) Bayramoglu, G. *J. Appl. Polym. Sci.* **2003**, *88*, 1843.
(43) Shi, Q.-H.; Tian, Y.; Dong, X.-Y.; Bai, S.; Sun, Y. *Biochem. Eng. J* **2003**, *16*, 317.

Table 1. Comparison of the Protein-Binding Capacity of Alumina−PHEMA−NTA−Cu^{2+} and Other Membrane Absorbers

membrane	thickness (μm)	surface area (cm^2)	pore size (μm)	porosity (%)	ligate	binding capacity (mg/cm^2)	binding capacity (mg/cm^3)
glass fiber[20]	8000	17.3	3	87	BSA	6.9	8.6
poly(acrylic acid) (polypropylene base polymer)[16]	150	3.14	0.4		lysozyme	0.3	20
cellulose[21]	64	125	0.2		BSA	0.027	4.2
PHEMA[a] (alumina support)	60	3.14	0.2	50	BSA	0.9	150

[a] This work.

filtering the BSA solution. We think that a thin layer of contaminants may quickly adsorb at the membrane surface. Elution with EDTA and/or regeneration with 0.1 M Cu^{2+} did not return the flow rate to 6.5 mL/min.

Table 1 compares the BSA-binding capacity of PHEMA−NTA−Cu^{2+}-coated alumina membranes with the capacities of several other membrane systems. Guo and Ruckenstein[20,44] modified glass fiber filters with trypsin or papain to bind proteins. They then packed 20 modified glass membrane filters (about 8 mm thick) into a cartridge and achieved an extremely high binding capacity of 6.9 mg of BSA/cm^2 of external membrane surface area. However, if one takes the membrane thickness into account and converts binding capacity into milligrams per cubic centimeter, the modified alumina membranes described here show a 17-fold higher capacity (compare rows 1 and 4 in Table 1). Recently, Ulbricht and Yang[16] used UV-initiated graft polymerization to grow poly(acrylic acid) from porous polypropylene microfiltration membranes. The resulting membranes showed a promising performance in adsorption of lysozyme by ion-exchange interactions (Table 1, row 2). Still, the capacity of those membranes was 7-fold lower than that described here. Kubota et al.[21] modified porous cellulose membranes with iminodiacetate−Cu^{2+} complexes, but those membranes (Table 1, row 3) gave only $^1/_{36}$ the binding capacity described here. The growth of brushes from alumina via ATRP provides an unusually productive method for introducing a high concentration of binding groups into membranes.

Elution of BSA and Reuse of Alumina−PHEMA−NTA−Cu^{2+} Membranes. In addition to rapid, high-capacity adsorption, elution and regeneration are also vital in the use of membrane absorbers.[45−47] Figure 5 shows results from multiple experiments comprising cycles of absorption of BSA, elution with 50 mM EDTA, and regeneration with 0.1 M Cu^{2+} on a single alumina−PHEMA−NTA−Cu^{2+} membrane. Within experimental error (<15%), there was no loss in binding amount over nine cycles, and >93% recovery of protein occurred in each cycle. The consistency in capacity over nine loadings implies that the elution buffer removed essentially all of the adsorbed protein from the membranes, even though the average calculated elution efficiency was only 94%. There likely was a systematic error in the analyses that resulted in a slight underestimation of elution efficiencies. Given the small volumes involved in the breakthrough experiments along with inaccuracies in the volume measurements and the need to integrate data such as those in Figure 3 to obtain adsorption amounts, this is certainly possible.

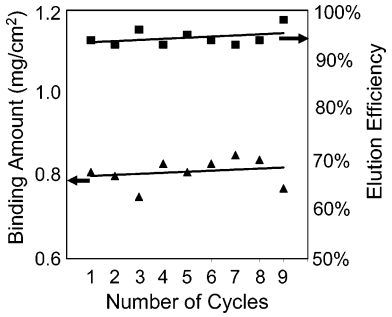

Figure 5. Binding amounts (▲) and elution efficiencies (■) for several cycles of BSA adsorption and elution followed by Cu^{2+} reloading of an alumina membrane modified with PHEMA−NTA. Flow rate, 0.9 mL/min; BSA concentration, 0.6 mg/mL; elution buffer, 50 mM EDTA, pH 7.2.

To more accurately assess elution efficiency, we passed 10 mL of 0.56 mg/mL BSA in pH 7.2 buffer through the membrane and analyzed this entire solution to determine how much BSA was adsorbed in the membrane. We also passed 5−10 mL of rinsing buffer through the membrane and determined the amount of protein in this effluent. Subtraction of the total amount of protein that came through the membrane from the amount of protein added to the initial 10 mL of BSA solution yielded the amount of bound BSA. (These experiments used mass rather than volume to more accurately determine the amount of solution passing through the membrane.) We eluted the protein with 10−15 mL of 0.1 M EDTA and analyzed the protein concentration in the entire solution. For three cycles of adsorption, elution, and Cu^{2+} binding, the average amount of BSA bound to the membrane was 0.78 ± 0.02 mg/cm^2, which is in reasonable agreement with the previous measurements. The elution efficiency was 101% ± 1%. Hence, essentially all of the protein is eluted.

Control experiments with membranes that were derivatized with PHEMA−NTA films but not exposed to Cu^{2+} showed elution of <0.02 mg/cm^2 BSA from a membrane loaded by a 0.56 mg/mL BSA solution and rinsed with buffer. These control experiments help to validate the experimental procedure and also indicate that the PHEMA−NTA films are not prone to high levels of nonspecific BSA adsorption under these conditions.

Adsorption of Myoglobin. We also examined the adsorption of myoglobin to alumina−PHEMA−NTA−Cu^{2+} membranes to see if molecular mass affects protein adsorption. BSA has a molecular mass of 67 kDa, an isoelectric point of 4.9, 17 histidine residues, and dimensions of 4.0 nm × 4.0 nm × 11.5 nm.[34] In contrast, myoglobin has a molecular mass of 17 kDa, an isoelectric point of 7.0, 11 histidine residues, and a size of 4.4 nm × 4.4 nm × 2.5 nm.[48] Figure

(44) Guo, W.; Ruckenstein, E. *J. Chromatogr. B* **2003**, *795*, 61.
(45) Avramescu, M.-E.; Girones, M.; Borneman, Z.; Wessling, M. *J. Membr. Sci.* **2003**, *218*, 219.
(46) Garipcan, B.; Andac, M.; Uzun, L.; Denizli, A. *React. Funct. Polym.* **2004**, *59*, 119.
(47) Kubota, N.; Kounosu, M.; Saito, K.; Sugita, K.; Watanabe, K.; Sugo, T. *J. Membr. Sci.* **1997**, *134*, 67.

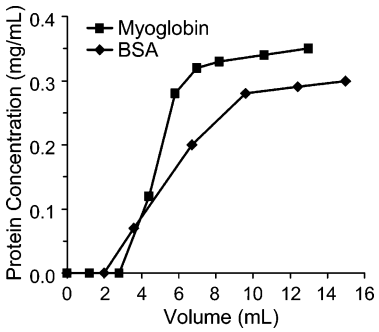

Figure 6. Breakthrough curves for adsorption of 0.3 mg/mL BSA and 0.35 mg/mL myoglobin on the same alumina−PHEMA−NTA−Cu^{2+} membrane. After adsorption of BSA, the membrane was regenerated with 0.05 M EDTA and 0.1 M Cu^{2+}.

6 shows the breakthrough curves for the two proteins on the same membrane. The membrane showed high binding capacities for both BSA (0.67 mg/cm^2, feed concentration 0.30 mg/mL) and myoglobin (0.50 mg/cm^2, feed concentration 0.35 mg/mL), but the breakthrough curve is sharper for myoglobin. Rapid myoglobin binding could be due to faster diffusion of this smaller protein in the brushes, but this needs further investigation. Future studies examining how the rate of binding varies with brush thickness and density should be helpful in this regard. (Brush thickness can be controlled by varying the polymerization time, while density can be controlled by changing the density of initiators.[37,49]) Another explanation for the rapid binding of myoglobin could be that the fraction of histidine residues in this protein is higher than in BSA.[40]

Conclusions

Metal-affinity membranes were prepared by ATRP of HEMA inside the pores of alumina substrates, followed by a series of derivatization steps to immobilize NTA−Cu^{2+} complexes. FESEM measurements confirmed the growth of PHEMA brushes inside the pores of alumina membranes, and reflectance FTIR spectroscopy verified the efficacy of the derivatization procedures. Equilibrium binding essentially followed the Langmuir isotherm, and the saturation binding capacity of PHEMA−NTA−Cu^{2+} for BSA was 150 mg/cm^3 of membrane. Moreover, saturation of the membrane with protein occurred in less than 15 min. After nine cycles of adsorption, elution, and regeneration, the membranes showed no detectable loss of capacity, and elution efficiencies were essentially 100%. The derivatized PHEMA brushes also showed rapid, high-capacity binding of myoglobin.

Acknowledgment. We thank the National Science Foundation (CHE-0316244) for financial support of this work. We also thank Dr. Baokang Bi and Dr. Per Askeland for their assistance in EDS and XPS studies.

Supporting Information Available: Reflectance FTIR spectra of PHEMA and PHEMA−SA films (3750−1250 cm^{-1}), energy-dispersive X-ray spectrum of PHEMA nanotubes, and UV−vis spectra from selected Bradford protein assays. This material is available free of charge via the Internet at http://pubs.acs.org.

CM060554M

(48) Kent, M. S.; Yim, H.; Sasaki, D. Y.; Satija, S.; Seo, Y.-S.; Majewski, J. *Langmuir* **2005**, *21*, 6815.

(49) Bao, Z.; Bruening, M. L.; Baker, G. L. *Macromolecules*, in press.